Acta Crystallographica Section A
Foundations of Crystallography
ISSN 0108-7673

Experimental study on the correlation lengths of the statistical dynamical theory of X-ray diffraction by measurements of integrated intensities from silicon crystals with dislocations

Daisuke Sakaki* and Toshihiko Takama

Division of Applied Physics, Graduate School of Engineering, Hokkaido University, Kita-ku, Sapporo 060-8628, Japan. Correspondence e-mail: sakaki@eng.hokudai.ac.jp

Received 2 July 2001
Accepted 2 October 2001

© 2002 International Union of Crystallography
Printed in Great Britain – all rights reserved

X-ray integrated intensities J were measured from Si single crystals containing dislocations as a function of crystal thickness using Mo $K\alpha$ radiation. The thickness dependence of J was compared with the statistical dynamical theory of Kato [*Acta Cryst.* (1980), A**36**, 763–769, 770–778], which contains three parameters: the static Debye–Waller factor E, the correlation length τ for the phase factor and the correlation length Γ for the wave-field amplitudes. These three parameters are absolutely required to interpret the experimental data in contrast to the case of γ-ray experiments in which J can be described by the parameter E alone. For our specimens, the ranges of the fitted values of τ and Γ are 0.003–0.108 μm and 2.4–7.3 μm, respectively, depending on the reflection plane and the crystal perfection. This fact indicates that the assumption made in Kato's original theory, that Γ is proportional to the extinction distance, should be abandoned. The reason for which the two correlation lengths can be neglected in the γ-ray experiments is clarified.

1. Introduction

Kato (1980*a*,*b*) developed the statistical dynamical theory of X-ray diffraction, which deals with the propagation of waves in randomly distorted crystals. A notable characteristic of this theory is that the primary and secondary extinctions are not separated in contrast to conventional diffraction theories. The theory is expected to explain diffraction phenomena from perfect to ideally imperfect crystals and may be used to correct for the extinction effect in crystals with any degree of imperfection and to characterize crystalline perfections. The effects of distortion on the diffraction are described by three parameters in the theory. They are the static Debye–Waller factor E, the correlation length of the phase factor τ and the correlation length of the wave-field amplitudes Γ. Kato (1980*a*,*b*) gave an analytical expression for the integrated intensity of X-ray diffraction for an incident spherical wave. A minor error in the theory was pointed out and revised by Al Haddad & Becker (1988) and Guigay (1989). Subsequently, Becker & Al Haddad (1989, 1990) discussed the magnitude of Γ and concluded that Γ is of the same order of magnitude as τ. This conclusion contradicts Kato's original assumption that Γ is proportional to the extinction distance.

The theory has been extended to interpret the angular profiles of diffraction observed using an incident plane wave by several authors (Bushuev, 1989*a*,*b*; Punegov, 1990; Pavlov & Punegov, 1998, 2000; Guigay & Vartanyants, 1999). The extended theories have been used to characterize crystals such as epitaxic films (Bushuev, 1989*a*; Punegov, 1990; Li *et al.*, 1995). However, there are a few extended theories that take the correlation length Γ into account (Pavlov & Punegov, 1998, 2000).

Several workers have performed experimental tests of the statistical dynamical theories (Olekhnovich *et al.*, 1983; Voronkov *et al.*, 1987; Schneider *et al.*, 1992; Takama & Harima, 1994; Kurbakov & Sokolov, 1999). Schneider *et al.* (1992) measured the absolute integrated intensities of γ-rays from Si single crystals with microdefects as a function of crystal thickness. The experimental data were compared with the theories by Kato (1980*a*,*b*) and by Becker & Al Haddad (1990). The result showed that the thickness dependence is explained by the static Debye–Waller factor E alone and the other parameters τ and Γ can be neglected in practice. Recently, Kurbakov & Sokolov (1999) applied the theories to the integrated intensities of γ-rays measured from SiO_2 single crystals with dislocations. The variation of the intensity with the reflection plane was again explained by the parameter E alone. On the other hand, Takama & Harima (1994) measured the integrated intensities from specimens similar to those used by Schneider *et al.* (1992) as a function of X-ray wavelength using white X-rays. The measurements showed that the wavelength dependence of the integrated intensity is not

Table 1
Specimens used for measurement.

Specimen no.	Thickness	Surface orientation	Dislocation density†
1	619 μm	[001]	0 cm/cm^3
2	652 μm	[1$\bar{1}$1]	600 cm/cm^3
3	583 μm	[001]	1.5 × 10^6 /cm^2

† Specimens 1 and 2 made by the Lang method and specimen 3 made by the etch-pit method.

interpreted by E alone, in contrast to the γ-ray case, and that the magnitudes of τ and Γ are several hundreds of Å and several micrometres, respectively.

The experimental tests have only been made on slightly distorted crystals. The tests made using γ-rays have shown a different result from those made using X-rays in regard to the correlation lengths τ and Γ. Moreover, the parameter Γ is neglected in the profile analyses using an incident plane wave. It seems therefore to be necessary to test Kato's theory for heavily distorted crystals and to clarify the reason for which the X-ray experiments gave a different result for the correlation lengths from that of γ-ray experiments. In the present study, we measure the integrated intensity from silicon single crystals with dislocations as a function of crystal thickness and compare the results with Kato's theory paying special attention to the correlation lengths.

2. Survey of the statistical dynamical theory

Kato's theory starts with taking the statistical average of the Takagi–Taupin equations (Takagi, 1962; Taupin, 1964) given by

$$\frac{\partial \langle D_o \rangle}{\partial s_o} = i\kappa_{-g} \langle \varphi D_g \rangle \tag{1a}$$

$$\frac{\partial \langle D_g \rangle}{\partial s_g} = i\kappa_g \langle \varphi^* D_o \rangle, \tag{1b}$$

where D_o and D_g are the amplitudes of the waves propagating in the incident direction with coordinate s_o and the diffracted direction with coordinate s_g, respectively. The reflection strength κ_g is given by $\lambda C F_g r_e / v$ (λ wavelength, C polarization factor = 1 for the σ state and $|\cos 2\theta_B|$ for the π state, F_g structure factor of g reflection, r_e classical radius of electron, v volume of unit cell). The lattice phase factor $\varphi(\mathbf{r})$ is defined by

$$\varphi(\mathbf{r}) = \exp[2\pi i \mathbf{g} \cdot \mathbf{u}(\mathbf{r})] = \langle \varphi \rangle + \delta\varphi(\mathbf{r}), \tag{2}$$

where $\mathbf{g}$ is the reciprocal-lattice vector and $\mathbf{u}(\mathbf{r})$ denotes the local lattice displacement from the undistorted position. The phase factor $\varphi(\mathbf{r})$ is expressed by the average $\langle \varphi \rangle = E$ and the deviation $\delta\varphi(\mathbf{r})$ from$\langle \varphi \rangle$. The average E is usually called the static Debye–Waller factor. The factor E is 1 for perfect crystals and zero for ideally imperfect crystals. Two kinds of correlation length are defined in the theory. One is the correlation length τ between the phase factors in an arbitrary direction given by

$$\tau = \int_0^\infty \langle \delta\varphi(0) \delta\varphi^*(z) \rangle (1 - E^2)^{-1} \, \mathrm{d}z. \tag{3}$$

The other is the correlation length Γ for the wave-field amplitudes (Kato, 1980*a*).

Kato (1980*b*) derived analytical expressions for the integrated intensity J in the symmetrical Laue case. According to Kato, the derived expression consists in the sum of the coherent, the incoherent and the mixed components. When one uses an unpolarized incident beam and a monochromator, J is given by

$$\begin{aligned} J &= K \exp(-\mu T)(R_\sigma + |\cos^2 2\theta_M \cos 2\theta_B| R_\pi)/2 \\ &= K \exp(-\mu T) R, \end{aligned} \tag{4}$$

where R_j ($j = \pi$ or σ) is the sum of the three components for the j state of polarization, θ_M the Bragg angle for the monochromator and μ the normal absorption coefficient for the crystal under consideration. The factor K includes the Bragg angle θ_B, wavelength, extinction distance and incident-beam intensity. It is noted that the factor K is independent of the crystal perfection for a given reflection.

The coherent component R_j^c for the j polarization has a relatively simple form given by

$$\begin{aligned} R_j^c &= EW[2ET/\Lambda_j] \exp[-2(1 - E^2) T\tau/\Lambda_j^2] \\ &\quad + E[I_0(2ET|F_g^i/F_g^r|/\Lambda_j) - 1] \exp[-2(1 - E^2) T\tau/\Lambda_j^2], \end{aligned} \tag{5}$$

where $W[x]$ $[= \int_0^x J_0(y)\,\mathrm{d}y]$ means the Waller integral of the zeroth-order Bessel function J_0, T the effective crystal thickness, I_0 the modified Bessel function of the zeroth order, Λ_j the extinction distance for the j polarization. F_g^r and F_g^i are the real and imaginary parts of the structure factor of the g reflection, respectively. It is seen that the coherent component includes the two parameters, E and τ, and is independent of Γ. The first term of R_j^c in (5) oscillates with T and corresponds to the *Pendellösung* oscillations. The second term corresponds to the Borrmann anomalous transmission. The incoherent component for the j polarization is expressed by

$$R_j^i = (1 - E^2)(\tau_e/\Lambda_j)^{-1} \sinh(2T\tau_e/\Lambda_j^2) \exp(-2T\tau_e/\Lambda_j^2), \tag{6}$$

where $\tau_e = (1 - E^2)\tau + E^2\Gamma$. The mixed component is rather complex and is not shown here. For $\tau = \Gamma = 0$, one can easily show that

$$\begin{aligned} R_j^c &= EW[2ET/\Lambda_j] + E[I_0(2ET|F_g^i/F_g^r|/\Lambda_j) - 1], \\ R_j^i &= T(1 - E^2)/\Lambda_j \quad \text{and} \quad R_j^m = 0. \end{aligned} \tag{7}$$

3. Experimental

Three parallel-sided Si single crystals were prepared. The thickness, surface orientation and dislocation density for each specimen are shown in Table 1. The density of as-grown dislocations was determined by taking Lang topographs or by counting etch-pit numbers. The integrated intensities J for the symmetrical Laue-case diffraction were measured as a function of the effective crystal thickness T, which was varied by

the ϕ-axis inclination method (Lawrence & Mathieson, 1977) using a four-circle goniometer. It is given by $T = t/(\cos\theta_B \cos\phi)$ for crystal thickness t. Mo $K\alpha$ X-rays monochromated by a graphite crystal were utilized for the incident beam. The diffracted intensities were measured by the ω-scan method with a step angle of 0.01° with the use of a cadmium zinc telluride solid-state detector (XR100-CZT, Amptek Inc.). The integrated intensity J at one ϕ setting was obtained by integrating a rocking curve after subtracting the background intensity. A scintillation monitor counter was used to correct for the fluctuation of the incident-beam intensity. The measured reflections were the 220, the 400 and the 440 reflections for specimens 1 and 3, and the 220 and the 440 for specimen 2.

4. Results

Fig. 1 shows the integrated intensities J observed from specimens 1 and 2 for the 220 reflection as a function of the inclination angle ϕ. In Fig. 1(a) for the dislocation-free specimen, one recognizes faint *Pendellösung* oscillations near $\phi = 0$. The decrease of the integrated intensities with increasing ϕ in Figs. 1(a) and 1(b) is due to the increase in X-ray absorption. The integrated intensity J is given by (4). For a perfect crystal with E = 1, R consists of the Waller integral and the Borrmann transmission term. Therefore, the constant factor K for a given reflection is determined by comparing the measured J for the dislocation-free specimen with the theoretical calculation. The atomic scattering factors measured by Saka & Kato (1986) and the normal absorption coefficient (Wagenfeld, 1962) were used for the correction. Hereafter, R is designated 'corrected intensity' and compared with the theory.

Examples of the corrected intensity R are shown in Fig. 2 as a function of the effective crystal thickness for the 220 and the 440 reflections. The intensities obtained from the positive and negative ϕ angles are plotted together. As seen in the figure, the two intensities at the same thickness for each specimen with dislocations are slightly different from each other, although the dislocation-free specimen gives almost the same intensities. This is considered to originate from the shift of the X-ray illumination area during the ϕ rotation. Actually, it was observed in the topographs and the etch-pit density that the

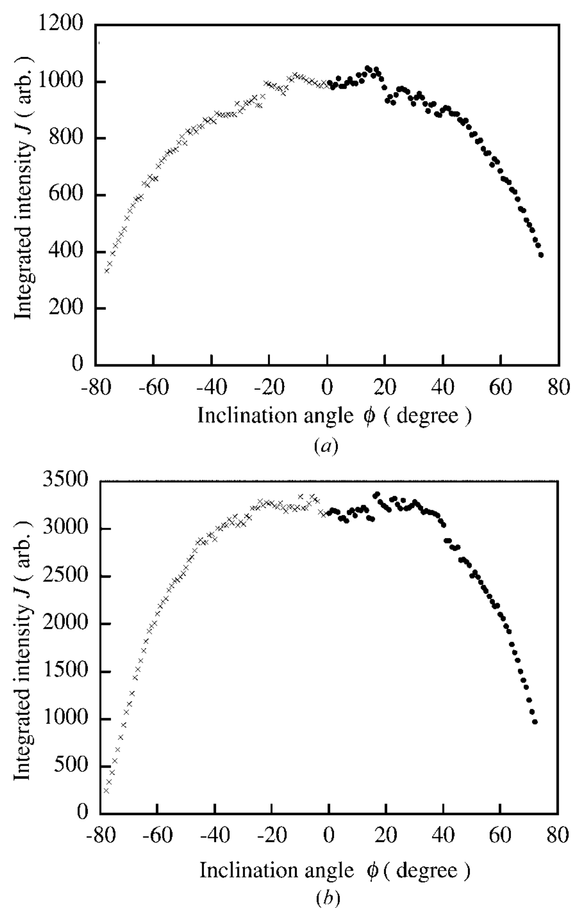

Figure 1
Examples of the measured integrated intensities J for the 220 reflection as a function of the inclination angle ϕ (a) for specimen 1 and (b) for specimen 2. Dots indicate measurements at positive angles and crosses at negative angles.

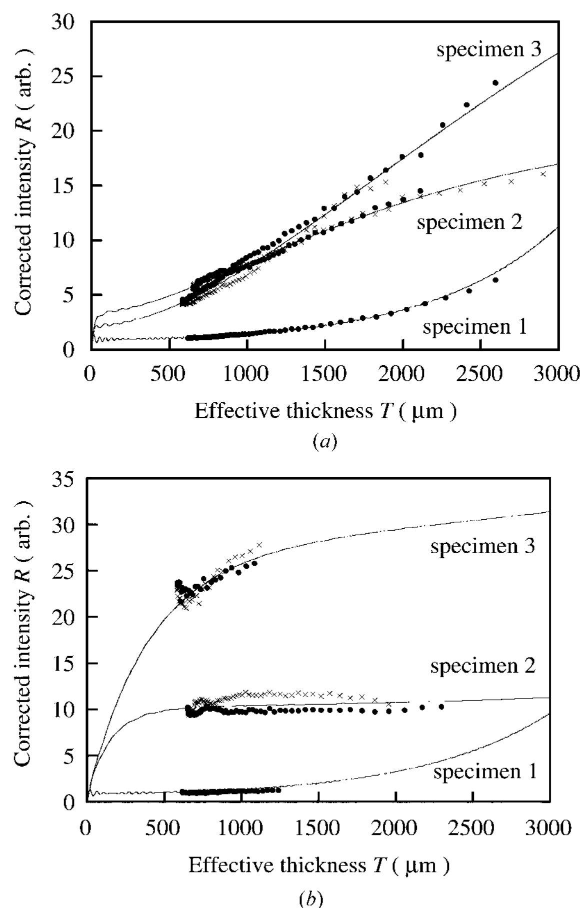

Figure 2
Corrected intensity R and results from fitting the theoretical integrated intensity to R using the three parameters (a) for the 220 reflection and b for the 440 reflection. Dots represent the observed intensities from positive values of ϕ and crosses from negative values. Lines show the best fit of theoretical R to the observed data introducing the three parameters of E, τ and Γ.

Table 2
Results from fitting the theoretical integrated intensity to the experiments assuming two models for the two parameters of τ and Γ.

Model 1 assumes that E, τ and Γ are free parameters. Model 2 assumes that τ and Γ are zero. E for specimen 1 is assumed to be 1. The r factor is defined by equation (8).

		Model 1				Model 2	
(*hkl*)	Specimen no.	E	τ (µm)	Γ (µm)	r (%)	E	r (%)
(220)	1	1	–	–	3.7	–	–
	2	0.4459 (3)	0.108 (2)	7.3 (1)	2.1	0.983(4)	16.5
	3	0.574 (4)	0.066 (4)	7.2 (6)	5.4	0.980 (1)	8.0
(400)	1	1	–	–	4.5	–	–
	3	0.424 (1)	0.028 (2)	5.9 (4)	3.4	0.980 (1)	28.5
(440)	1	1	–	–	4.8	–	–
	2	0.46 (2)	0.003 (1)	3.3 (4)	5.7	0.952 (1)	32.8
	3	0.321 (1)	0.050 (1)	2.4 (2)	3.8	0.796 (4)	12.6

dislocation density changes from area to area in the specimens. It is seen in Fig. 2 that the corrected intensities of R observed from the distorted specimens for the 220 reflection increase with the effective thickness. The R for the 440 from specimen 2, however, is almost constant in the range of T between 0.6 and 2.3 mm. The slope of the increase depends on the specimen and the reflection plane.

5. Comparison with the theory

As stated in the introduction, the correlation lengths τ and Γ could be neglected in γ-ray experiments (Schneider *et al.*, 1992; Kurbakov & Sokolov, 1999). On the other hand, they could not be ignored in the X-ray case (Takama & Harima, 1994). In the following, the present results are compared with Kato's theory assuming two models for the two correlation lengths. In the comparison, the R values obtained for the positive and negative ϕ angles are used simultaneously.

In the first model, the three parameters E, τ and Γ are assumed to be free. The theoretical intensity $R_{\rm the}$ is fitted to the observed data $R_{\rm obs}$. The examples of the comparisons are presented in Fig. 2. Table 2 summarizes the best-fitted values of the parameters and the r factors defined by

$$r = \frac{\sum |R_{\rm obs} - R_{\rm the}|}{\sum R_{\rm obs}} \times 100\,(\%). \qquad (8)$$

The values of E range from 0.321 to 0.574 and those of τ and Γ from 0.003 to 0.108 µm and 2.4 to 7.3 µm, respectively. The obtained r values are distributed in the range 2.1–5.7%. This model explains well the observed intensity variations.

In the second model, E is taken as a free parameter while τ and Γ are assumed to be zero according to the result by Schneider *et al.* (1992). Fig. 3 displays examples of fitting for the 220 and 440 reflections. $R_{\rm the}$ for the 220 reflection of specimen 3 agrees relatively well with the experiment, while $R_{\rm the}$ for the 440 reflection shows very poor agreement. Generally speaking, $R_{\rm the}$ in the second model shows a monotonic increase with increasing effective thickness. This is understood from (7), which indicates a linear increase of R_j^i with T. The best fitted values of E and the r factors are shown in Table 2. As a natural consequence, the obtained E values totally differ from those of the first model. The second model shows poor agreement in comparison with the first model as evidenced by the large r values.

6. Discussion

Takama & Harima (1994) tested the theory by measuring the integrated intensities as a function of X-ray wavelength. This test used Si single crystals with heat-induced microdefects for the samples to show that the three parameters, E, τ and Γ, are required to explain the experimental results and that the values of τ and Γ were 0.05–0.09 µm and 0.07–0.5 µm, respectively. The present value of τ (0.003–0.108 µm) is similar to the previous one and Γ (2.4–7.3 µm) is about one order of magnitude longer. By considering this fact and the above discussions, one can say that the three parameters are necessary to explain the intensities from distorted crystals in X-ray experiments. Kato

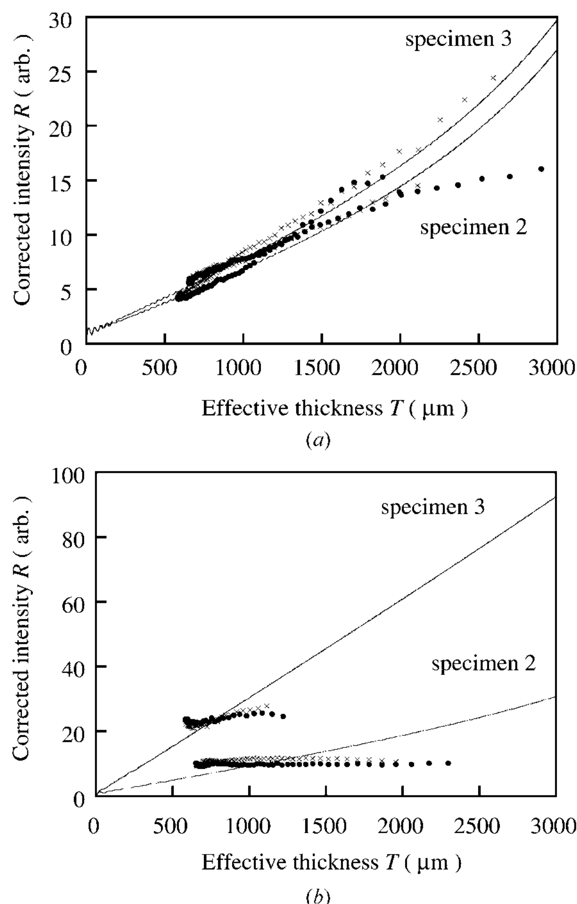

Figure 3
Comparison between the corrected intensity R and the theoretical one using only E as a free parameter (a) for the 220 reflection and (b) for the 440 reflection. Dots represent the observed intensities from positive values of ϕ and crosses from negative values. Lines show the best fit of the theoretical curve for R to the observed data using E alone.

assumed that Γ is close to Λ/E. The present values of Λ range from 19 μm for the 440 reflection to 12 μm for the 220, which give 27–60 μm for Kato's Γ. Thus, one can conclude that Γ is not so long as Kato assumed.

The present results show that the diffracted X-ray intensity from a distorted crystal can be explained by the use of three parameters. If one uses radiations with shorter wavelengths, what thickness dependence would be observed for the same specimen? We discuss here the difference in intensity for the Mo $K\alpha$ radiation (0.707 Å) and the ^{192}Ir γ-radiation of wavelength 0.0392 Å used by Schneider *et al.* (1992). All three parameters E, τ and Γ are assumed to be inherent in a given specimen and reflection and to be independent of wavelength. The 400 reflection of our specimen 3 is taken as an example. Curve (1) in Fig. 4 displays the best-fitted profile calculated for the Mo $K\alpha$ radiation using the three parameters. The optimal values are 0.424 for E, 0.028 μm for τ and 5.9 μm for Γ. If γ-radiation is used instead of Mo $K\alpha$, curve (2) should be observed for this specimen with the same three parameters. A striking difference is noticed between curves (1) and (2). The calculated intensity for the γ-radiation varies almost linearly with the crystal thickness.

Next, we try to approximate curve (2) using only the E parameter assuming $\tau = 0$ and $\Gamma = 0$ for the γ-radiation. Curve (3) in Fig. 4 is an approximation of curve (2). The fitted E value of 0.495 is slightly different from the result using three parameters in the fit. There are no significant differences between curves (2) and (3). This indicates that the integrated intensity observed with γ-radiation is insensitive to τ and Γ as pointed out by Schneider *et al.* (1992). Kato's theory contains the parameters τ and Γ with the form divided by the extinction distance Λ. The extinction distance for the ^{192}Ir γ-radiation is 18 times as long as that for the Mo $K\alpha$ radiation. This leads to the linear increase in intensity of the incoherent component in the γ-ray experiment. The parameter τ is directly related to crystal imperfections such as the size, form and density of defects. Therefore, one can say that an X-ray experiment gives more useful information in general about distortion in crystals than a γ-ray experiment.

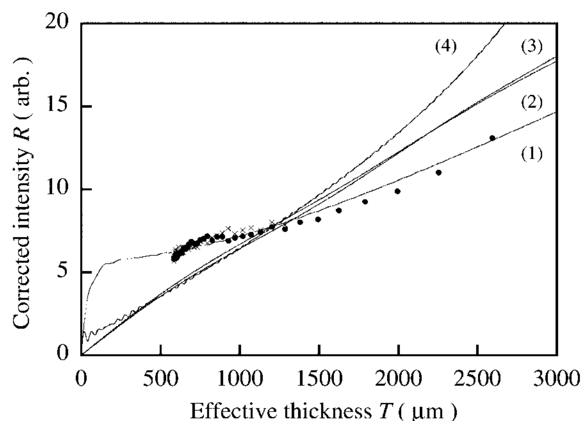

Figure 4
Fits of various theoretical intensities of R to experimental data for the 400 reflection of specimen 3. Curve (1) is the best fit using the three parameters for Mo $K\alpha$. Curve (2) is the calculation using the same values of the three parameters as curve (1) for γ-radiation with wavelength of 0.0392 Å. Curve (3) shows the fit for R, calculated using the E parameter alone, to the curve (2) for γ-radiation. Curve (4) displays the best fit to the observed R using E and τ for Mo $K\alpha$ radiation.

The statistical dynamical formulations developed for an incident plane wave have been used to characterize crystal perfections in artificial multilayer films (Bushuev, 1989*a*; Punegov, 1990; Li *et al.*, 1995). The profiles of rocking curves observed using the double-crystal method were analyzed using the developed theories. In these formulations, the correlation length τ depends on the deviation from the exact Bragg incidence. The functional form of τ is calculated according to a model of crystal distortions. In usual analyses, τ includes the thickness and inclination of the layers and displacement of the unit cell. Results of the analysis would provide information about the distortion. However, the correlation length Γ was neglected *a priori* in all the investigations. Curve (4) in Fig. 4 shows a best fit to the observed intensity for the Mo $K\alpha$ radiation assuming $\Gamma = 0$ (E and τ are free). The parameters E and τ are exactly the same as the ones obtained from model 2 described above. The calculated intensity does not agree with the experimental data. Generally speaking, the variation of the diffracted intensity for large crystal thickness cannot be explained by neglecting Γ as seen in Figs. 3 and 4. The parameter Γ should be taken into account in a full analysis, and also in a profile analysis.

7. Summary

In the present study, we measured the integrated intensities from Si crystals with and without dislocations as a function of crystal thickness. The intensities from the dislocated crystals did not increase linearly with thickness but remained constant for large crystal thicknesses. Kato's theory explained well the thickness dependence if E, τ and Γ were assumed to be free parameters. It was confirmed that the parameters τ and Γ could not be neglected in contrast to the case of the γ-ray experiments.

A computer simulation was made in order to clarify the reason for the difference in τ and Γ values between X-ray and γ-ray measurements. It was found that the γ-ray diffracted intensity is insensitive to τ and Γ in comparison with the case for X-rays because of the large extinction length for γ-rays. This indicates that X-ray diffraction is more useful in obtaining information on crystal distortion than γ-ray diffraction.

The authors would like to thank Professor H. Hashizume of Nara Institute of Science and Technology for helpful suggestions and a critical reading of the manuscript.

References

Al Haddad, M. & Becker, P. J. (1988). *Acta Cryst.* A**44**, 262–270.
Becker, P. J. & Al Haddad, M. (1989). *Acta Cryst.* A**45**, 333–337.
Becker, P. & Al Haddad, M. (1990). *Acta Cryst.* A**46**, 123–129.
Bushuev, V. A. (1989*a*). *Sov. Phys. Solid State*, **31**, 1877–1882.
Bushuev, V. A. (1989*b*). *Sov. Phys. Crystallogr.* **34**, 163–167.

Guigay, J. P. (1989). *Acta Cryst.* A**45**, 241–244.
Guigay, J. P. & Vartanyants, I. A. (1999). *J. Phys. D: Appl. Phys.* **32**, A84–A87.
Kato, N. (1980*a*). *Acta Cryst.* A**36**, 763–769.
Kato, N. (1980*b*). *Acta Cryst.* A**36**, 770–778.
Kurbakov, A. & Sokolov, A. (1999). *Acta Cryst.* A**55**, 259–266.
Lawrence, J. L. & Mathieson, A. McL. (1977). *Acta Cryst.* A**33**, 288–293.
Li, M., Mai, Z., Li, J., Li, C. & Cui, S. (1995). *Acta Cryst.* A**51**, 350–353.
Olekhnovich, N. M., Karpei, A. L., Olekhnovich, A. I. & Puzenkova, L. D. (1983). *Acta Cryst.* A**39**, 116–122.
Pavlov, K. M. & Punegov, V. I. (1998). *Acta Cryst.* A**54**, 214–218.
Pavlov, K. M. & Punegov, V. I. (2000). *Acta Cryst.* A**56**, 227–234.
Punegov, V. I. (1990). *Sov. Phys. Crystallogr.* **35**, 336–340.
Saka, T. & Kato, N. (1986). *Acta Cryst.* A**42**, 469–478.
Schneider, J. R., Bouchard, R., Graf, H. A. & Nagasawa, H. (1992). *Acta Cryst.* A**48**, 804–819.
Takagi, S. (1962). *Acta Cryst.* **15**, 1311–1312.
Takama, T. & Harima, H. (1994). *Acta Cryst.* A**50**, 239–246.
Taupin, D. (1964). *Bull. Soc. Fr. Minéral. Cristallogr.* **87**, 469–511.
Voronkov, S. N., Piskunov, D. I., Chukhovskii, F. N. & Maksimov, S. K. (1987). *Sov. Phys. JETP*, **65**, 624–629.
Wagenfeld, H. (1962). *J. Appl. Phys.* **33**, 2907–2908.